

SUB-BARRIER FUSION OF DRIP-LINE NUCLEI

K. HAGINO

*Institute for Nuclear Theory, Department of Physics,
University of Washington, Box 351550, Seattle, WA 98195, USA
E-mail: hagino@phys.washington.edu*

A. VITTURI

*Dipartimento di Fisica, Università di Padova and INFN, Padova, Italy
E-mail: andrea.vitturi@pd.infn.it*

We discuss the role of break-up process of a loosely-bound projectile in subbarrier fusion reactions. Coupled-channels calculations are carried out for $^{11}\text{Be} + ^{208}\text{Pb}$ and $^4\text{He} + ^{238}\text{U}$ reactions by discretizing in energy the particle continuum states. Our calculations show that the coupling to the break-up channel has two effects, namely the loss of flux and the dynamical modulation of fusion potential. Their net effects differ depending on the energy region. At energies above the Coulomb barrier, the former effect dominates over the latter and cross sections for complete fusion are hindered compared with the no coupling case. On the other hand, at below the barrier, the latter effect is much larger than the former and complete fusion cross sections are enhanced consequently.

1 Introduction

Many questions concerning the effects of break-up process on subbarrier fusion have been raised during the last few years both from the experimental^{1,2,3,4,5,6} and theoretical^{7,8,9,10} points of view. The issue has become especially relevant in recent years due to the increasing availability of radioactive beams. These often involve weakly-bound systems close to the drip lines for which the possibility of projectile dissociation prior to or at the point of contact cannot be ignored.

One interesting question is whether the break-up process hinders or enhances fusion cross sections. In addressing this, it is vital to specify which quantity is being compared with which quantity; otherwise a comparison is meaningless. The latter quantity is rather obvious in theoretical calculations, because one can artificially switch on and off couplings to the break-up channel. When we refer in this paper to that break-up enhances/hinders fusion cross sections, it will be in this sense unless we mention explicitly. As for the former quantity, there are two possibilities, namely complete fusion cross sections or the sum of complete and incomplete fusion cross sections. From studies of fusion of stable nuclei where break-up process is not important, we have learned that any coupling of the relative motion of the colliding nuclei

to nuclear intrinsic excitations causes large enhancements of the fusion cross section at subbarrier energies over the predictions of a simple barrier penetration model.¹¹ It may not be difficult to imagine that the same thing happens to the break-up channel as well; cross sections for inclusive processes, i.e., the sum of complete and incomplete fusion cross sections would be enhanced by couplings to the break-up channel. On the other hand, one could also argue intuitively that break-up process removes a part of flux and thus cross sections for complete fusion would be hindered. As will be shown below, fusion cross sections are determined by the competition of these two mechanisms.

In passing, this sort of consideration is relevant also when one discusses experimental data and compares them with theoretical calculations. For instance, it is important to bear in mind that the recent Padova/RIKEN data³ as well as the Canberra data,⁴ which used ${}^9\text{Be}$ beams, contain both the complete and incomplete fusion cross sections for the neutron break-up channel (${}^9\text{Be} \rightarrow n + {}^8\text{Be}$), while they are only the complete fusion cross sections with respect to the α -break-up channel (${}^9\text{Be} \rightarrow \alpha + {}^5\text{He}$ or $2\alpha + n$).

In the past, different theoretical approaches to the problem have led to controversial results, not only quantitatively but also qualitatively. Hussein *et al.* derived a local dynamical polarization potential V_{DPP} for break-up process and computed complete fusion cross sections as⁷

$$\sigma_{\text{CF}} = \frac{\pi}{k^2} \sum_l (2l+1) P_F^{(0)} \exp\left(\frac{2}{\hbar} \int_{-\infty}^{\infty} dt W(r(t))\right), \quad (1)$$

where $P_F^{(0)}$ is the fusion probability *in the absence of break-up*, k is the wave number in the entrance channel, and $W(r)$ is the imaginary part of the dynamical polarization potential V_{DPP} . The integral in the exponent is evaluated along the classical trajectory $r(t)$, where $r(t=0)$ corresponds to the distance of closest approach. The idea of this formalism is that the effects of break-up can be well described in terms of the survival probability $P_{\text{surv}} = 1 - P_{\text{bu}} = \exp(2 \int W(r) dt/\hbar)$. Since $W(r)$ is negative, the break-up process always hinders complete fusion cross sections in this formalism. Subsequently, Takigawa *et al.* pointed out that the classical trajectory used by Hussein *et al.* corresponded to the one for scatterings, and for fusion reactions the time integral should have been from $-\infty$ to 0.⁸ Consequently the effects of break-up were moderated over the estimate made by Hussein *et al.*, but the qualitative conclusion remained the same. These conclusions were later criticized by Dasso and Vitturi. They performed coupled-channels calculations by treating the break-up channels as a single state and obtained totally different results, i.e., enhancement of complete fusion cross sections due to the break-up.⁹

What would be the origin of these apparently controversial results? We argue that the coupling to the break-up channel leads to the dynamical modification of fusion potential as in fusion of stable nuclei. At subbarrier energies, this effect is most relevant, leading to the enhancement of complete fusion cross section. Such effects are automatically included in the coupled-channels formalism. The dynamical modulation of fusion potential is related to the real part of a dynamical polarization potential, which both Hussein *et al.* and Takigawa *et al.* completely threw away. Therefore, if the real part of the polarization potential is properly taken into account, their formalism would provide an enhancement of complete fusion cross sections at energies below the Coulomb barrier. Actually, Ref. 12 shows that it is indeed the case, although their calculations are not satisfactory in a sense of Takigawa *et al.*⁸ and a full calculation within their formalism has still been awaited.

Another origin of the controversy might be the simplified assumption used by Dasso and Vitturi. As mentioned above, the entire continuum space was mocked up by a single discrete configuration,⁹ and therefore the main feature of continuum couplings were not entirely included. This would underestimate the break-up effects, especially those effects, if any, which remove the incident flux.

From this point of view, in this paper, we repeat similar calculations as of Dasso and Vitturi, but by considerably increasing the number of continuum states.¹³ We also use microscopic form factors in contrast to the previous studies, where form factors were assumed to have an exponential form. These two aspects enable us to describe simultaneously the dynamics of continuum couplings inside and outside the Coulomb barrier, leading to a more conclusive result on the effects of break-up process on subbarrier fusion. In the next section, we review briefly the coupled-channels formalism and define the complete and incomplete fusion cross sections. The specific applications of the formalism to $^{11}\text{Be} + ^{208}\text{Pb}$ and $^4,6\text{He} + ^{238}\text{U}$ are given in the following section 3.

2 Coupled-Channels Formalism for Subbarrier Fusion of Drip-Line Nuclei

Our aim is to discuss effects of the break-up of the projectile nucleus on subbarrier fusion reactions by solving coupled-channels equations. The coupled-channels equations in the isocentrifugal approximation are given by¹⁴

$$\left[-\frac{\hbar^2}{2\mu} \frac{d^2}{dr^2} + \frac{l(l+1)\hbar^2}{2\mu r^2} + V_N^{(0)}(r) + \frac{Z_P Z_T e^2}{r} + \epsilon_n - E \right] \psi_n(r) = - \sum_m F_{nm}(r) \psi_m(r), \quad (2)$$

where the angular momentum of the relative motion in each channel has been replaced by the total angular momentum l .¹⁵ In eq. (2), $V_N^{(0)}$ is the nuclear potential in the entrance channel, and ϵ_n is the excitation energy of the n -th channel. Here, we assume that $n = 0$ labels the ground state of the projectile nucleus and the all other n refer to particle continuum states, which are associated with the break-up channels. It is straightforward to include bound excited states of the projectile and/or the excitations in the target nucleus. F_{nm} are the coupling form factors, which we compute on the microscopic basis. It is to fold the external nuclear and Coulomb fields with the proper single-particle transition densities, obtained by promoting the last weakly-bound nucleon to the continuum states. More explicitly, the single-particle form factor for the promotion from the bound state $(n_1 \ell_1 j_1 m_1)$ to the continuum state $(\ell_2 j_2 m_2)$ with continuum energy E assumes the form

$$\begin{aligned}
& F_{n_1 \ell_1 j_1 m_1 \rightarrow E \ell_2 j_2 m_2}(r) = \\
& = \sqrt{\pi} \sum_{\lambda} (-1)^{m_2 + \frac{1}{2}} \delta(\ell_1 + \ell_2 + \lambda, \text{even}) \left\langle j_1 \frac{1}{2} j_2 - \frac{1}{2} \middle| \lambda 0 \right\rangle \\
& \times \frac{\sqrt{2j_1 + 1} \sqrt{2j_2 + 1}}{\sqrt{2\lambda + 1}} \langle j_1 - m_1 j_2 m_2 | L(m_2 - m_1) \rangle \sqrt{\frac{2\lambda + 1}{4\pi}} \delta_{m_1, m_2} \\
& \times \left[\int_0^{\infty} r'^2 dr' \int_{-1}^{+1} du R_{E \ell_2 j_2}^*(r') R_{n_1 \ell_1 j_1}(r') V_T(\sqrt{r^2 + r'^2 - 2rr'u}) P_{\lambda}(u) \right] (3)
\end{aligned}$$

The functions $R_{E \ell_2 j_2}(r)$ and $R_{n_1 \ell_1 j_1}(r)$ are the single particle wave functions for the continuum and bound states, respectively. The potential V_T is the mean field felt by the single particle due to the presence of the target, responsible of the transition, not to be confused therefore with the projectile mean field generating the single particle wave functions. This potential obviously involves both a nuclear and a Coulomb component. Note that for long ranged transition densities, as in the case of a weakly bound system, the resulting Coulomb formfactor will differ from the pure $r^{-\lambda-1}$ form much outwards than in the traditional case of stable systems. See Ref. [16] for more details.

The coupled-channels equations (2) are solved by imposing the incoming wave boundary condition (IWBC), where there are only incoming waves at r_{min} which is taken somewhere inside the Coulomb barrier.^{14,17} The boundary conditions are thus expressed as

$$\begin{aligned}
\psi_n(r) & \rightarrow T_n \exp\left(-i \int_{r_{min}}^r k_n(r') dr'\right) & r \leq r_{min}, & (4) \\
& \rightarrow H_l^{(-)}(k_n r) \delta_{n,0} + R_n H_l^{(+)}(k_n r) & r > r_{max}, & (5)
\end{aligned}$$

where

$$k_n(r) = \sqrt{\frac{2\mu}{\hbar^2} \left(E - \epsilon_n - \frac{l(l+1)\hbar^2}{2\mu r^2} - V_N^{(0)}(r) - \frac{Z_P Z_T e^2}{r} \right)} \quad (6)$$

is the local wave number for the n -th channel and $k_n = \sqrt{2\mu(E - \epsilon_n)/\hbar^2}$. $H_l^{(-)}$ and $H_l^{(+)}$ are the incoming and the outgoing Coulomb functions, respectively.

The fusion probability is defined as the ratio between the flux inside the Coulomb barrier and the incident flux. For our boundary conditions given by eqs. (4) and (5), it reads

$$P_n = \frac{k_n(r_{min})}{k_0} |T_n|^2 \quad (7)$$

for the n -th channel. Complete fusion is a process where all the nucleons of the projectile are captured by the target nucleus. We thus define cross sections of complete fusion using the flux for the non-continuum channel (i.e., $n=0$) as¹⁸

$$\sigma_{\text{CF}} = \frac{\pi}{k_0^2} \sum_l (2l+1) P_0 = \frac{\pi}{k_0^2} \sum_l (2l+1) \frac{k_0(r_{min})}{k_0} |T_0|^2. \quad (8)$$

The flux for the particle continuum channel ($n \neq 0$) are associated with incomplete fusion, whose cross sections we define as

$$\sigma_{\text{ICF}} = \frac{\pi}{k_0^2} \sum_l (2l+1) \sum_{n \neq 0} P_n = \frac{\pi}{k_0^2} \sum_l (2l+1) \sum_{n \neq 0} \frac{k_n(r_{min})}{k_0} |T_n|^2. \quad (9)$$

3 Results

3.1 The $^{11}\text{Be} + ^{208}\text{Pb}$ reaction

We now apply the coupled-channels formalism presented in the previous section to fusion of drip-line nuclei. We first consider the fusion reaction $^{11}\text{Be} + ^{208}\text{Pb}$, where the projectile is generally regarded as a good example of a single neutron ‘halo’. In a pure single-particle picture, the last neutron in ^{11}Be occupies the $2s_{1/2}$ state, bound by about 500 keV. The strong concentration of strength at the continuum threshold evidenced in break-up reactions¹⁹ has been mainly ascribed to the promotion of this last bound neutron to the continuum of $p_{3/2}$ and $p_{1/2}$ states at energy E_c via the dipole field.^{19,20} Since the presence of the first excited $1p_{1/2}$ state (still bound by about 180 keV) may perturb the transition to the corresponding $p_{1/2}$ states in the continuum,²¹

we prefer here to consider only the contribution to the $p_{3/2}$ states. The couplings to the $p_{1/2}$ states are certainly not negligible, but we expect that they will simply further enhance the effects on the fusion cross section and therefore will not alter our qualitative conclusions. The initial $2s_{1/2}$ bound state and the continuum $p_{3/2}$ states are generated by Woods-Saxon single-particle potentials whose depths have been adjusted to reproduce the correct binding energies for the $1p_{3/2}$ and $2s_{1/2}$ bound states. In particular, one needs for the latter case a potential which is much deeper than the “standard” one. As we mentioned in the previous section, the form factor $F(r; E_c)$ as a function of the internuclear separation r and of the energy E_c in the continuum is then obtained by folding the corresponding transition density with the external field generated by the target. In addition to the Coulomb field, a Woods-Saxon nucleon-nucleus potential is used, with parameters of $R = r_0 A_T^{1/3}$, $r_0 = 1.27$ fm, $a = 0.67$ fm, $V = (-51 + 33 (N - Z)/A)$ MeV, and $V_{ls} = -0.44V$.

Selected cuts of the form factor $F(r; E_c)$ are shown in Figure 1. The individual contribution arising from the Coulomb and nuclear interactions are shown separately. In Fig. 1 (a), we display the form factor as a function of r for a fixed value of the energy in the continuum (E_c being 0.9 MeV). Note the long tail of the nuclear contribution as a consequence of the large radial extension of the weakly-bound wave function, resulting in the predominance of the nuclear form factor up to the unusual distance of about 25 fm. The same reason gives rise to a deviation of the Coulomb part from the asymptotic behaviour $1/r^2$. Note also, due to the negative $E1$ effective charge of the neutron excitation, the constructive interference of the nuclear and Coulomb parts. In figs. 1 (b) and 1 (c), we show, instead, the energy dependence of the form factor at fixed value of r . While at large r the curves are peaked at very low energies, reflecting the corresponding $B(E1)$, at smaller distances around the barrier, for values which are more relevant to the fusion process, the peaks of the distributions move to higher energies, in particular for the nuclear part. Hence, the sudden approximation employed in Refs. 7 and 8, where the energy of continuum states E_c was all set to be zero, is not justified.

In order to perform the coupled-channel calculation, the distribution of continuum states is discretized in bins of energy, associating to each bin the form factor corresponding to its central energy. We have considered the continuum distribution up to 2 MeV, with a step of 200 keV. In this way, the calculations are performed with 10 effective excited channels. We have checked the convergence concerning the maximum energy of the continuum states included in the calculation, and found that it is rather slow. We have, however, found that our main conclusions again do not qualitatively change provided that the maximum excitation energy of the continuum states is at least 2 MeV, as con-

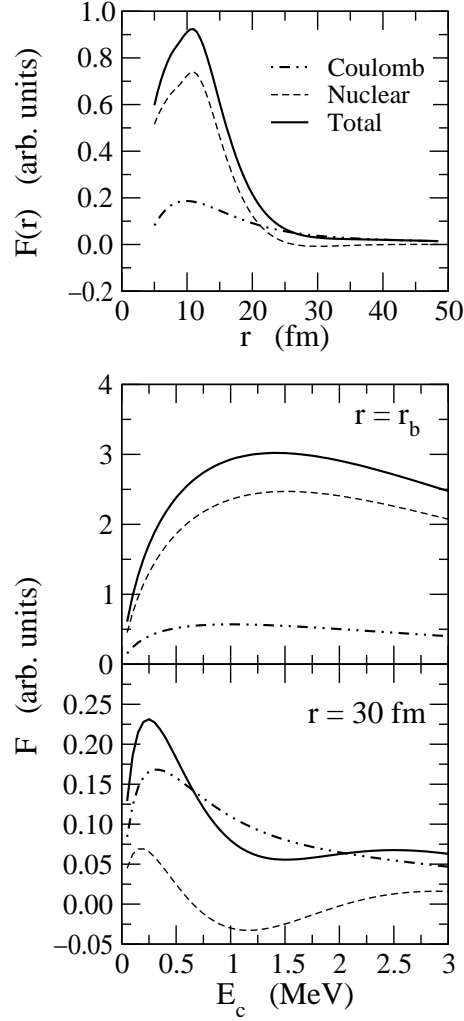


Figure 1: Coupling form factor $F(r; E_c)$ associated with the dipole transition in ^{11}Be from the neutron bound state $2s_{1/2}$ ($E_b = -500$ keV) to the continuum state $p_{3/2}$ with energy E_c . In (a) the Coulomb (the dash-dotted line), nuclear (the dashed) and total (the solid) form factors are shown as a function of r at the continuum energy $E_c = 0.9$ MeV. In (b) and (c) the form factors are shown as a function of the energy E_c in the continuum for $r = r_{\text{barrier}} = 11.6$ fm and $r = 30$ fm, respectively.

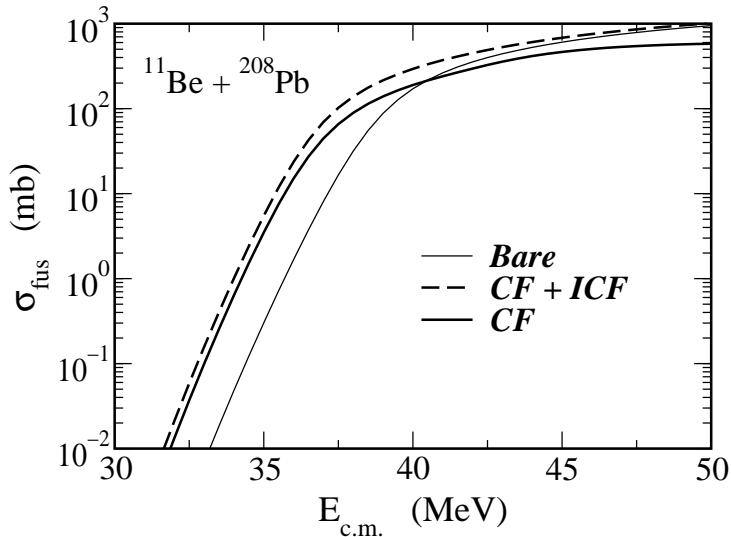


Figure 2: Fusion cross section for the reaction $^{11}\text{Be} + ^{208}\text{Pb}$ as a function of the bombarding energy in the center of mass frame. The thin solid curve shows the results of the one-dimensional barrier penetration as a reference. The solid and the dashed lines are solutions of the coupled-channels equations for the complete fusion and the complete plus incomplete fusion, respectively.

sidered in this work. The ion-ion potential is assumed to have a Woods-Saxon form with parameters $V_0 = -152.5$ MeV, $r_0 = 1.1$ fm and $a = 0.63$ fm, a set that leads to the same barrier height as the Akyüz-Winther potential.

In the previous theoretical studies of fusion of drip-line nuclei, ^{7,8,9} the excitations to the “soft-dipole mode” of the projectile were also included in the calculations and the effects of the break-up were thus somewhat perturbed. In the present calculations, in order to isolate the genuine effect of the break-up process, we include only the continuum states in the coupling scheme, neglecting continuum-continuum coupling as well as other inelastic channels such as bound excited states in either reaction partner. For the same reason, we do not take into account static modifications on the ion-ion potential which may arise from the halo properties of the projectile.²² Our calculations, therefore, only attempt to give qualitative indications. They will, however, still reveal interesting aspects of effects of couplings of the ground to continuum states on subbarrier fusion.

Figure 2 shows the results of our calculations. The solid line represents

the cross section of complete fusion, leading to ^{219}Rn , while the dashed line denotes the sum of the complete and incomplete fusion cross sections. Also shown for comparison, by the thin solid line, is the cross section in the absence of the couplings to the continuum states. One can see that they enhance the fusion cross sections at energies below the barrier over the predictions of a one-dimensional barrier penetration model. Note that this is the case not only for the total (complete plus incomplete) fusion probability, but also for the complete fusion in the entrance channel. This finding supports the results of the original calculation performed in Ref. 9. As it has been emphasized there, accounting properly for the dynamical effects of the coupling in the classically forbidden region is essential to arrive at this conclusion.

The situation is completely reversed at energies above the barrier. Fusion in the break-up channel becomes more important and dominates at the expense of the complete fusion. As a consequence, the cross sections for complete fusion are hindered when compared with the no-coupling case.

3.2 The $^{4,6}\text{He} + ^{238}\text{U}$ reactions

We next consider the fusion reactions $^{4,6}\text{He} + ^{238}\text{U}$. This is partly motivated by the recent measurement by the SACLAY group.⁶ They compared the fusion cross sections of these two systems and concluded that the cross sections for the ^6He projectile were systematically larger than those for the ^4He projectile, both below and above the Coulomb barrier. One might think that this conclusion is inconsistent with ours discussed in the previous subsection as well as with the experimental observation of the Canberra group⁴ that the break-up hinders complete fusion cross sections at energies above the Coulomb barrier. However, the situation is somewhat more complicated since the experimental data of the SACLAY group⁶ likely include both the complete and incomplete fusion cross sections, and also since the halo structure of ^6He may alter significantly the static fusion potential. We therefore decided to carry out coupled-channels calculations for these systems in order to clarify the role played by the break-up of the ^6He projectile.

To this end, we describe the structure of ^6He using the di-neutron cluster model as in Ref. 23. The potential between the di-neutron and α particle is determined so as to reproduce the correct binding energy of ^6He . The ground state is assumed to be the $2s$ state in this potential. In the coupled-channels calculations, we include continuum states with $L = 1$ and $L = 2$ spins. To construct these wave functions, we slightly adjust the depth of the potential for $L = 2$ so as to reproduce the correct resonance state at 1 MeV. We include the continuum states up to $E_c = 5$ MeV with energy step of 0.25 MeV. As for the

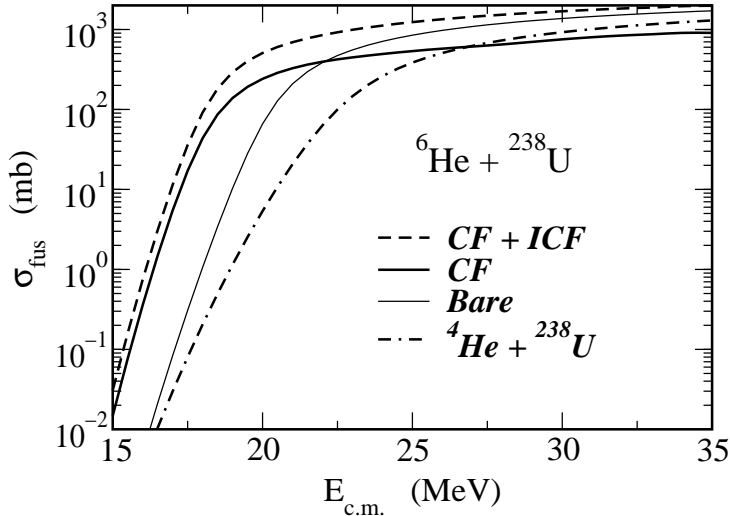


Figure 3: Same as fig.2, but for the ${}^6\text{He} + {}^{238}\text{U}$ reaction. The meaning of each line is the same as in fig.2 except for the dot-dashed line, which denotes fusion cross sections for the ${}^4\text{He} + {}^{238}\text{U}$ system.

bare potential, we use the Woods-Saxon potential with $V_0 = -174.05$ MeV, $r_0=1.01$ fm, and $a=0.67$ fm for the ${}^4\text{He} + {}^{238}\text{U}$ system. The potential for the ${}^6\text{He} + {}^{238}\text{U}$ system is constructed with the folding procedure using the same di-neutron cluster model. For simplicity, we neglect the deformation effects of the ${}^{238}\text{U}$ target which would influence the both reactions in a similar way, although one definitely has to include them when one compares theoretical fusion cross sections with the experimental data.

Figure 3 shows the theoretical fusion cross sections for the ${}^6\text{He} + {}^{238}\text{U}$ reaction and their comparison with the ${}^4\text{He} + {}^{238}\text{U}$ system. The relation between the complete fusion cross sections (the solid line) and the bare cross sections (the thin solid line) within the ${}^6\text{He} + {}^{238}\text{U}$ system is qualitatively the same as that in the ${}^9\text{Be} + {}^{208}\text{Pb}$ system discussed in the previous subsection; the coupling to the break-up channels enhances the complete fusion cross sections at energies below the barrier and hinders them at above the barrier energies. The cross sections for the ${}^4\text{He}$ projectile are denoted by the dot-dashed line. The figure shows that the complete fusion cross sections for the ${}^6\text{He} + {}^{238}\text{U}$ reaction are even smaller than the cross sections for the ${}^4\text{He}$ projectile at energies above the Coulomb barrier. Notice that the sum of the complete and incomplete fusion cross sections for the ${}^6\text{He}$ projectile is always

larger than the cross sections for the ^4He projectile, that reminisces the experimental observation by the SACLAY group.⁶ It would thus be interesting, but perhaps experimentally challenging, to isolate the contribution from the complete fusion in the $^6\text{He} + ^{238}\text{U}$ system.

4 Summary

We have performed exact coupled-channels calculations for weakly-bound systems using realistic coupling form factors to discuss effects of break-up on subbarrier fusion reactions. As examples, we have considered the fusion of ^{11}Be with a ^{208}Pb target as well as the $^{4,6}\text{He} + ^{238}\text{U}$ fusion reactions. We found that the coupling to break-up channels enhances cross sections for the complete fusion at energies below the Coulomb barrier, while it reduces them at energies above.

Very recently, a complete fusion excitation function was measured for the $^9\text{Be} + ^{208}\text{Pb}$ reaction at near-barrier energies by Dasgupta *et al.*⁴ They showed that cross sections for complete fusion are considerably smaller at above-barrier energies compared with a theoretical calculation that reproduces the total fusion cross section. Also, the fusion cross sections for the $^{4,6}\text{He} + ^{238}\text{U}$ systems measured by the SACLAY group⁶ seem to indicate that the break-up effects enhance fusion cross sections at energies below the barrier. These two recent experiments are in general agreement with our results.

Acknowledgments

We thank C.H. Dasso and S.M. Lenzi for discussions. The work of K.H. was supported by the U.S. Dept. of Energy under Grant No. DE-FG03-97ER4014.

References

1. J. Takahashi *et al.*, *Phys. Rev. Lett.* **78**, 30 (1997).
2. K.E. Rehm *et al.*, *Phys. Rev. Lett.* **81**, 3341 (1998).
3. C. Signorini *et al.*, *Eur. Phys. J. A* **2**, 227 (1998).
4. M. Dasgupta *et al.*, *Phys. Rev. Lett.* **82**, 1395 (1999).
5. J.J. Kolata *et al.*, *Phys. Rev. Lett.* **81**, 4580 (1998); P.A. De Young *et al.*, *Phys. Rev. C* **58**, 3442 (1998); E.F. Aguilea *et al.*, *Phys. Rev. Lett.* **84**, 5058 (2000).
6. M. Trotta *et al.*, *Phys. Rev. Lett.* **84**, 2342 (2000).
7. M.S. Hussein, M.P. Pato, L.F. Canto and R. Donangelo, *Phys. Rev. C* **46**, 377 (1992).

8. N. Takigawa, M. Kuratani and H. Sagawa, *Phys. Rev. C* **47**, R2470 (1993).
9. C.H. Dasso and A. Vitturi, *Phys. Rev. C* **50**, R12 (1994).
10. K. Yabana, *Prog. Theo. Phys.* **97**, 437 (1997).
11. M. Dasgupta, D.J. Hinde, N. Rowley, and A.M. Stefanini, *Annu. Rev. Nucl. Part. Sci.* **48**, 401 (1998); A.B. Balantekin and N. Takigawa, *Rev. Mod. Phys.* **70**, 77 (1998).
12. M.S. Hussein, M.P. Pato, L.F. Canto and R. Donangelo, *Phys. Rev. C* **47**, 2398 (1993).
13. K. Hagino, A. Vitturi, C.H. Dasso, and S.M. Lenzi, *Phys. Rev. C* **61**, 037602 (2000).
14. K. Hagino, N. Rowley, and A.T. Kruppa, *Comp. Phys. Comm.* **123**, 143 (1999).
15. K. Hagino, N. Takigawa, A.B. Balantekin, and J.R. Bennett, *Phys. Rev. C* **52**, 286 (1995).
16. C.H. Dasso, S.M. Lenzi and A. Vitturi, *Nucl. Phys. A* **639**, 635 (1998).
17. S. Landowne and S.C. Pierper, *Phys. Rev. C* **29**, 1352 (1984).
18. K. Hagino and N. Takigawa, *Phys. Rev. C* **58**, 2872 (1998).
19. T. Nakamura *et al.*, *Phys. Lett. B* **331**, 296 (1994); T. Nakamura *et al.*, *Phys. Lett. B* **394**, 11 (1997).
20. H. Esbensen, G.F. Bertsch and C.A. Bertulani, *Nucl. Phys. A* **581**, 107 (1995).
21. C.H. Dasso, S.M. Lenzi and A. Vitturi, *Phys. Rev. C* **59**, 539 (1999).
22. N. Takigawa and H. Sagawa, *Phys. Lett. B* **265**, 23 (1991).
23. K. Rusek and K.W. Kemper, *Phys. Rev. C* **61**, 034608 (2000).